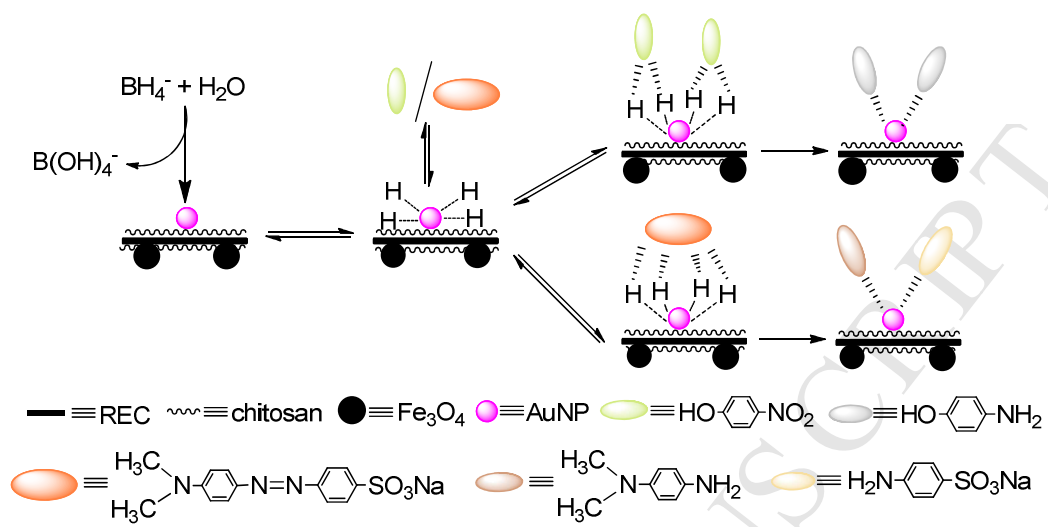


Graphic abstract



Preparation and catalytic properties of magnetic rectorite-chitosan-Au composites

Rufei Zhang^a, Pengwu Zheng^b, Xiaofei Ma^{a,*}

^a Chemistry Department, School of Science, Tianjin University, Tianjin 300072,
China

^b School of Pharmacy, Jiangxi Science and Technology Normal University, Nanchang,
Jiangxi 330013, China

Author Information

*Corresponding author; E-mail address: maxiaofei@tju.edu.cn (X.F. Ma);

Tel.: +86 22 27406144; fax: +86 22 27403475.

Abstract

A novel composite was assembled by introducing magnetic Fe_3O_4 nanoparticles, chitosan and Au nanoparticles (AuNPs) on rectorite (REC) surfaces. The obtained REC- Fe_3O_4 -CTS-Au composite was characterized and used as the catalyst to remove 4-nitrophenol (4-NP) and methyl orange (MO) from water in the presence of NaBH_4 . The large surface of REC and the abundant hydroxyl group of chitosan on REC surface could restrain the agglomeration of AuNPs. REC- Fe_3O_4 -CTS-Au exhibited the superiority in catalytic efficiency. At the catalyst dosage of 150 mg/L, it took only 15 min for 0.2 mM 4-NP solution to reach complete reduction, and 30 min for 1.0 mM 4-NP solution. This catalyst had the higher catalytic activity for 4-NP than MO reduction. Moreover, the catalyst could be conveniently separated and recycled from the reaction mixtures using an external magnetic field, and reused for 4-NP (or MO) reduction in fourteen cycles with retaining the original 99% (or 95%) conversion efficiency. This work indicates that REC- Fe_3O_4 -CTS-Au can be a promising catalyst for the highly efficient degradation of organic dyes.

Keywords: Rectorite; gold; catalyst; 4-nitrophenol; methyl orange

1. Introduction

Rectorite (REC) is a regularly layered silicate clay mineral comprised of dioctahedral mica-like layer and dioctahedral smectite-like layer in a ratio of 1:1 [1]. It has attracted a great deal of attention due to its unique properties, such as high temperature resistance, good dispersion in water, cation exchange ability, adsorption capacity and adjustable interlayer spacing [2-4]. The large surface area and cation exchange ability of REC make it a promising candidate for catalyst support in chemical reaction.

Noble metal nanoparticles (NPs) possess fascinating physicochemical properties such as optical, electronic, magnetic and biomedical properties, which are extensively used in catalysis, organic synthesis, storage of hydrogen, biomedical sensors, drug delivery, and wastewater treatment. Therefore, noble metal NPs have rapidly attracted great attention in the past decade. [5-9] Among various metal nanoparticles, gold nanoparticles (AuNPs) have been considered as an attractive and promising catalyst due to their good recyclability, non-toxic property and excellent catalytic performance at low temperature. Ismail et al. [10] reported the photochemical deposition of Au onto mesoporous TiO₂ and excellent catalytic activity of the catalyst was confirmed. Yu et al. [11] synthesized the gold-deposited porous anodic aluminum oxide (AAO) membranes, which showed high catalytic activity towards reduction of 4-nitrophenol by NaBH₄. Besides, AuNP/poly(methyl methacrylate) beads [12], gold nanoparticle-graphene hybrids [13], Au-Pd nanoparticles/graphene oxide [14], graphene oxide aerogels loaded with Au/Pd nanoparticles [15] were also reported to have excellent

catalytic performance. Among all the AuNP-catalyzed reactions, catalytic reaction of 4-nitrophenol to 4-aminophenol in the presence of sodium borohydride (NaBH_4) has become one of the most widely used model reactions owing to the complete conversion without by-products and easy measurement of both reactants and products by UV-Vis spectroscopy [16].

However, significant defects of metal nanoparticles still exist, such as low catalytic efficiency due to the agglomeration and difficult separation etc. It is a major and urgent issue to improve the catalytic activity and utilization efficiency of nano-materials. Hydroxyl groups of chitosan could form interaction with gold ions and restrain the agglomeration of AuNPs to enhance the dispersion and catalytic activity of AuNP catalyst [17-19].

With the growing interest in the textile industry, particularly the dye-containing waste-water and their industrial discharge was reported as one of the major sources of water pollution worldwide. These dyes may cause permanent injury to the eyes of humans and animals, and even 4-nitrophenol (4-NP) on inhalation and ingestion may cause liver and kidney damage [6, 20, 21].

In this work, REC was selected as the support of AuNPs and chitosan intercalated REC layers with ion exchange method to improve its specific surface area. Magnetic Fe_3O_4 NPs were also introduced into the catalyst composites for easy recovery. On REC surface, hydroxyl groups of chitosan (CTS) could form interaction with gold ions and restrain the agglomeration of Au nanoparticles to enhance the dispersion and catalytic activity of AuNP catalyst. The reductions of 4-NP and methyl

orange (MO) were designed as the model reaction to evaluate the catalytic activity and efficiency of magnetic Au catalyst composites. The project will set a scientific foundation for the study of metal nanoparticle supports with large surface area as well as the recycle and efficiency improvement of metal catalysts.

2. Experimental

2.1. Materials

Sodium rectorite was purchased from Hubei Zhongxiang Rectorite Mine (Wuhan, China). All other reagents were of analytical grade and commercially available.

2.2 Preparation of magnetic REC composite

1 g REC was added to a 200 mL solution of 1.17 g $\text{FeCl}_3 \cdot 6\text{H}_2\text{O}$ and 0.6 g $\text{FeSO}_4 \cdot 7\text{H}_2\text{O}$. 20 mL $\text{NH}_3\text{H}_2\text{O}$ solution (8 M) was added dropwise to produce iron oxide at 60 °C under N_2 . The pH of the final suspension was about 12. The mixture was held at 70 °C for 4 h, and then washed with distilled water. The obtained REC- Fe_3O_4 composite was dried at 100 °C for 3 h.

2.3. Fabrication of REC- Fe_3O_4 -CTS composite

1 g REC- Fe_3O_4 was added to 50 mL distilled water under ultrasonication for 10 min to obtain REC- Fe_3O_4 suspension. 0.3 g chitosan was added into 30 mL distilled water and HCl was then added to get a chitosan solution at pH=2. The REC- Fe_3O_4 suspension and chitosan solution were mixed and agitated at room temperature for 30 min. REC- Fe_3O_4 -CTS composite was obtained after washing with water several times and drying.

2.4. Preparation of REC-Fe₃O₄-CTS-Au composite

1 g REC-Fe₃O₄-CTS composite dispersed in distilled water (50 mL) under ultrasonication for 10 min. 15 mL 1% HAuCl₄ solution was mixed with 12 mL polyvinyl pyrrolidone (PVP) (1 mg/L) as the surfactant, and the mixture was added to the REC suspension. 8 mL 0.01 mol/L NaOH solution was mixed with 0.24 g NaBH₄ and then added dropwise to the above-mentioned mixture at 90°C for 5 min to form the composites. The mixture was cooled to room temperature, washed with distilled water and ethanol, and vacuum-dried at 50°C for 4 h to get REC-Fe₃O₄-CTS-Au composites.

The fabrication process of the catalyst composites was exhibited in Fig. 1.

2.5. Scanning electron microscope (SEM) and Transmission electron microscope (TEM)

REC, REC-Fe₃O₄, REC-Fe₃O₄-CTS and REC-Fe₃O₄-CTS-Au composites were stabilized in a sample holder with conducting resin, coated with gold, and observed with an S-4800 scanning electron microscope.

REC-Fe₃O₄ and REC-Fe₃O₄-CTS-Au powders were dispersed in alcohol. Sample suspensions were dropped into a copper grid, dried in air, and tested with a JEM-2100F transmission electron microscope.

2.6. X-ray diffraction (XRD)

X-ray diffraction patterns of REC, REC-Fe₃O₄, REC-Fe₃O₄-CTS and REC-Fe₃O₄-CTS-Au were recorded in reflection mode in the range of 1-80° (2θ) at room temperature with a D/MAX-2500 operated at a CuKα wavelength of

1.542Å.

2.7. Fourier transform infrared spectroscopy (FTIR)

FTIR analysis of REC, REC-Fe₃O₄, REC-Fe₃O₄-CTS and REC-Fe₃O₄-CTS-Au were performed on a BIO-RAD FTS3000 IR spectra scanner. The grinded sample powders were dispersed in KBr and pressed into transparent sheets for testing.

2.8. Thermogravimetric analysis (TG)

Thermal properties of REC, REC-Fe₃O₄, REC-Fe₃O₄-CTS and REC-Fe₃O₄-CTS-Au were measured with a ZTY-ZP thermal analyzer. Samples were heated from room temperature to 800°C at a heating rate of 10°/min in nitrogen atmosphere.

2.9. Specific surface area

The specific surface area of REC, REC-Fe₃O₄, REC-Fe₃O₄-CTS and REC-Fe₃O₄-CTS-Au were measured with an Autosorb-1 specific surface area analyzer (Quantachrome Instruments, USA) using the BET method on the base of N₂ adsorption data.

2.10 Magnetic property of REC-Fe₃O₄-CTS-Au

The magnetic property of REC-Fe₃O₄-CTS-Au was measured on a vibrating sample magnetometer (LDJ 9600-1, LDJ Electronics Inc., USA).

2.11 Catalytic activity study of REC-Fe₃O₄-CTS-Au for 4-NP and MO

1, 3 or 6 mg REC-Fe₃O₄-CTS-Au was respectively dispersed in 20 mL 4-NP (or MO) aqueous solution containing 0.02 g NaBH₄. The dosage of

REC-Fe₃O₄-CTS-Au was 50, 150 or 300 mg/L. The mixture was added and shaken on a rotary shaker at 100 rpm at 30°C for a certain period of time. REC-Fe₃O₄-CTS-Au was magnetically separated from the solution. The concentration of residual 4-NP (or MO) were measured using UV-Vis spectrophotometer [22]. To evaluate the catalytic capacity of the REC-Fe₃O₄-CTS-Au, the initial concentration of 4-NP changed from 0.2 to 1.0 mmol/L (i.e. 27.8, 55.6, 83.4, 111.3, 139 mg/L), and the initial concentration of MO changed from 0.03 to 0.09 mmol/L (i.e. 10, 20, 30 mg/L).

To measure the recyclability, 3 mg REC-Fe₃O₄-CTS-Au and 0.02 g NaBH₄ were added to 20 mL aqueous solution, and shaken on a rotary at 100 rpm for 30 min. After REC-Fe₃O₄-CTS-Au was separated from the solution with the magnet, the residual 4-NP (or MO) was determined with UV-Vis spectrometry. Afterwards, REC-Fe₃O₄-CTS-Au was used for a second catalysis run and the similar catalytic process was repeated fourteen times. The concentrations of 4-NP and MO were 0.4 mmol/L and 0.06 mmol/L, respectively.

3. Results and discussion

3.1 Characterization of the composites

Fig. 2 (a) revealed that REC was composed of the plates with the size of about 20 μm × 20 μm. In Fig. 2 (b), REC-Fe₃O₄ exhibited Fe₃O₄ particles covering the REC sheets. Since Fe³⁺ and Fe²⁺ could be adsorbed onto the REC surface, Fe₃O₄ particles formed on the transparent plates of REC with the size of 10-40 nm, as shown in Fig. 2 (e). In Fig. 2 (c), some thin REC plates were

observed, which could be related to the intercalation of acidified chitosan into REC plates. As shown in Fig. 2 (d) and (f), the scattered gold nanoparticles with a diameter of below 10 nm were loaded on the surface of REC-Fe₃O₄. The good dispersion of gold nanoparticles was also achieved, which was ascribed to the interaction of polyhydroxy groups of chitosan [23, 24]. As REC-Fe₃O₄-CTS-Au could be easily recovered by magnetic field, this composite without obvious agglomeration of AuNP could achieve better catalytic efficiency and thus was more preferred.

In Fig. 3 (a), raw REC exhibited strong R(001) and R(002) diffraction pattern at $2\theta=4.10^\circ$ and 8.11° , respectively. Based on the Bragg diffraction equation, $2d\sin\theta=\lambda$, the distance between the REC interlayers was calculated to be about 2.16 and 1.09 nm. After being modified by Fe₃O₄ and acid-treated chitosan, the R(001) patterns shifted to 4.00° and 3.62° for REC-Fe₃O₄ and REC-Fe₃O₄-CTS, and the interlayer distance increased to 2.26 and 2.44 nm, respectively. For the XRD pattern of REC-Fe₃O₄-CTS, the R(001) reflection of REC was obviously reduced, and the intensity of the R(002) reflection was absent. Since REC had a swelling property similar to that of montmorillonite (Mt) [25], the interlayer Na⁺ of Mt-like layers in REC could easily exchange with the -NH₃⁺ cation parts of chitosan, and chitosan intercalated the REC layers [19]. For REC-Fe₃O₄-CTS-Au, both R(001) and R(002) diffraction peaks were absent, which could be attributed to the partial damage of REC's orderly structure in the process of modification (i.e. mostly the intercalation or even exfoliation of REC

layers) [18].

In the XRD pattern (Fig. 3 (b)), REC-Fe₃O₄ displayed distinct peaks at 2 θ values of about 30.1, 35.6, 43.3, 57.1 and 62.7. These positions and relative peak intensities corresponded to the characteristic peaks of Fe₃O₄ [1]. In the XRD spectra of REC-Fe₃O₄-CTS-Au, the peaks at 38.2°, 44.3°, 64.7°, 77.9° were ascribed to face-centered cubic (fcc) bulk gold of (111), (200), (220), (311), respectively, which were in accordance with the standard values in the standard XRD card of gold (JCPDS 04-784) [26]. These peaks confirmed the successful loading of gold nanoparticles onto REC layers.

Fig. 4 (a) exhibited the FTIR spectra of REC and composites. With regard to REC, the peaks at 3638 cm⁻¹ was attributed to the hydroxyl stretching band of Si-O-H. The peak at 1021 cm⁻¹ was related to the in-plane Si-O-Si stretching vibration and the peaks at 819 and 701 cm⁻¹ were associated with Si-O-Al bending and Al-O-out-of-plane. The above peaks appeared in the spectra of REC composites, as well. The broad and intense band of REC-Fe₃O₄ at 3450 cm⁻¹ was due to stretching vibrations of hydroxyl groups from iron oxide [27]. In addition, with the introduction of acid-treated chitosan, the broad stretching vibration of N-H and the stretching vibration band of -CH₂- group at 2935 cm⁻¹ could be easily observed in the spectra of REC-Fe₃O₄-CTS and REC-Fe₃O₄-CTS-Au composites [28].

The thermogravimetric (TG) curves of REC and composites were shown in Fig. 4 (b). The decomposed temperature of chitosan was about 300°C with about 51.7 wt% mass loss, and REC-Fe₃O₄-CTS showed a weight loss of about 8 wt% at the

decomposed temperature of chitosan. The quantity of chitosan was calculated by matching the percentage weight loss of REC-Fe₃O₄-CTS to the percentage of weight loss of chitosan at the decomposed temperature. The content of chitosan in REC-Fe₃O₄-CTS was estimated to be about 15.5 wt%. When gold nanoparticles were loaded on REC-Fe₃O₄-CTS, the mass loss of REC-Fe₃O₄-CTS-Au decreased to about 7% at about 300°C. If it was supposed that no chitosan was lost during the process of loading Au nanoparticles, the decreased mass loss derived from the loading of Au nanoparticles. The content of Au was calculated to be about 14.3 wt%, by matching the percentage weight loss (7 wt%) of REC-Fe₃O₄-CTS-Au to the decreased percentage (1 wt%) of weight loss of chitosan.

The BET surface area of REC was 10.43 m²/g, while the BET surface area of REC-Fe₃O₄ was 77.46 m²/g, much higher than that of raw REC. The increased surface area of REC-Fe₃O₄ was attributed to the new-generated nanoscale Fe₃O₄ particles. When chitosan was introduced, the decline in surface area (53.71 m²/g) of REC-Fe₃O₄-CTS was due to the attachment of polymer on the surface of REC-Fe₃O₄. However, the nanoscale Au particles only resulted in the slight improvement of surface area (55.96 m²/g) of REC-Fe₃O₄-CTS-Au. This could be ascribed to the partial embedding of AuNPs in chitosan polymers because of the good interaction between AuNPs and chitosan [23, 24].

Fig. 5 showed the magnetization of REC-Fe₃O₄-CTS-Au as a function of the applied magnetic field at 300 K. Magnetization increased with an increase in the magnetic field. REC-Fe₃O₄-CTS-Au possessed good magnetic properties with the

saturation magnetization (5.83 emu/g) and exhibited an extremely small hysteresis loop and low coercivity (14.0 Oe), as is typically characteristic of superparamagnetic particles [10].

3.2 Catalytic mechanism

The possible catalytic mechanism for the reduction of 4-NP and MO with the catalysis of REC-Fe₃O₄-CTS-Au was presented in Fig. 6. The 4-NP reduction by NaBH₄ in aqueous solution catalyzed by AuNP could be explained by the Langmuir-Hinshelwood (LH) model [29]. The reaction between the adsorbed 4-NP and the Au-H bonds is the rate-limiting step, compared with the fast diffusion of the reactants, i.e. borohydride and 4-NP. According to Fig. 6, the first step involved the hydrolysis of NaBH₄ to yield active hydrogen; afterwards, the active hydrogen was transformed and adsorbed onto the surface of AuNP; finally, 4-NP reacted with the active H-bond on the surface of AuNP to produce 4-aminophenol. Similarly, MO reacted with the active H-bond to produce N,N-dimethylaniline and sodium sulfanilate by breaking N=N bond of MO. In comparison, the numbers of catalyzed NP was two times as much as that of MO on the surface of one Au particle.

3.3. Catalytic properties of REC-Fe₃O₄-CTS-Au catalyst

Fig. 7 reveals the effect of contact time on the reduction of 4-NP and MO over REC-Fe₃O₄-CTS-Au catalyst in aqueous media at 30°C. Fig. 7 (a) provided a clear color changes from light yellow (or dark yellow) to colorless for 4-NP (or MO) with the catalytic times. REC-Fe₃O₄-CTS-Au could be well dispersed in

water to catalyze 4-NP (or MO), and this magnetic composite could be easily recovered with the magnet.

In Fig. 7 (b) for the reduction of 0.4 mmol/L 4-NP, the absorbance of 4-NP at 400 nm decreased rapidly accompanied by an increase of adsorption peak at 300 nm, which was ascribed to the reducing product, 4-aminophenol. After 25 min, the characteristic peak at 400 nm of 4-NP disappeared, which suggested the complete catalysis of 4-NP. This indicated that under mild condition the reduction of 4-NP could achieve a high yield with REC-Fe₃O₄-CTS-Au as catalyst. In contrast, the porous 3D Au/graphene monolith could catalyze 0.1 mmol/L 4-NP completely within 25 min [30] and the quaternized chitosan/AgNP nanocomposite film could catalyze 0.2 mmol/L 4-NP completely within 45 min [31]. Therefore, REC-Fe₃O₄-CTS-Au exhibited the superiority in catalytic efficiency.

In Fig. 7 (c) for the degradation of MO, the absorbance of MO at 465 nm decreased rapidly accompanied by an increase of adsorption peak at about 248 nm, which related to the combined absorbance from the degraded products (N, N-dimethylaniline at 243 nm and sodium sulfanilate at 250 nm). After 30 min, the characteristic peak at 465 nm of MO disappeared due to the complete catalysis of MO.

To evaluate the catalytic activity of REC-Fe₃O₄-CTS-Au, the reaction kinetics of the reduction of 4-NP and MO were studied. The reaction processes could be described with the dependence of the absorbance (at 400 nm for 4-NP

and 465 nm for MO) on the contact time. The adopted pseudo-first-order kinetic model is expressed as follows [31]:

$$\frac{dC_t}{dt} = \ln\left(\frac{C_t}{C_0}\right) = \ln\left(\frac{A_t}{A_0}\right) = -k_{app}t$$

where C_0 is the initial concentration of 4-NP (or MO), C_t is the concentration of 4-NP (or MO) at any time (t). A_0 is the absorbance of 4-NP (or MO) at $t=0$, A_t is the absorbance at any time (t). The apparent rate constant, k_{app} , is corresponded to the catalytic rate, i.e. the higher the apparent rate constant is, the higher the catalytic rate is. Measured from the linear plot of $\ln(A_t/A_0)$ versus time, according to Fig. 7 (b and c), the rate constant (k_{app}) value was 0.15 and 0.06 min^{-1} , and the catalytic process fit pseudo-first-order kinetic model well with correlation coefficient $R > 0.99$. The results indicated that the catalyst possessed the higher catalytic activity for 4-NP than MO reduction. On the one hand, according to catalytic mechanism, MO degradation consumed more the active H atoms than 4-NP reduction. On the other hand, due to the larger molecular volume, MO diffused on the catalyst surface more difficultly than 4-NP.

3.4 Effect of the catalyst dosages and dye concentrations on the reduction

As shown in Fig. 8, the effect of REC- Fe_3O_4 -CTS-Au dosage and 4-NP concentration on the reduction of 4-NP was illustrated in the presence of NaBH_4 . At the same catalyst dosage, 4-NP solution with the lower concentration required less time to reach complete reduction. At the catalyst dosage of 50 mg/L, the complete reduction took place within 20 min for 0.2 mM 4-NP solution, while only 70% 4-NP reduction occurred in 30 min for 1.0 mM solution. The catalytic

efficiency tended to increase while varying the concentration of catalyst from 50 to 300 mg/L. At the catalyst dosage of 150 mg/L, it took only 15 min for 0.2 mM 4-NP solution to reach complete reduction, and 30 min for 1.0 mM 4-NP solution. However, the catalytic efficiency increased slowly as the catalyst dosage increased from 150 mg/L to 300 mg/L. Thus, the optimal catalyst dosages are approximately 150 mg/L for 4-NP reduction.

The influence of catalyst dosage and MO concentration on the degradation of MO was revealed in Fig. 9. Since the catalytic activity for MO was lower than 4-NP, MO solutions with the lower concentration (0.03 to 0.09 mM) were catalyzed. At the catalyst dosage of 50 mg/L for 30 min, only 77% MO degraded for 0.09 mM solution, and about 90% MO degraded for 0.06 mM solution. When the dosages increase to 150 mg/L, about 90% MO degradation occurred in 30 min. When REC-Fe₃O₄-CTS-Au dosage was increased to 300 mg/L, above 95% MO degraded in less 25 min. To catalyze MO solution with higher concentration, more REC-Fe₃O₄-CTS-Au catalyst was required to achieve the high catalytic efficiency (e.g. 95%).

3.5 The recyclability of REC-Fe₃O₄-CTS-Au

The recyclability test in Fig. 10 (a) showed that complete conversion (99% of conversion efficiency of 4-NP to 4-aminophenol in 30 min) could be achieved after fourteen cycles with the catalysis of REC-Fe₃O₄-CTS-Au. Similarly, REC-Fe₃O₄-CTS-Au catalyst could be successfully reused for MO degradation in fourteen runs with keeping the original 95% conversion efficiency in Fig. 10

(b). Since no obvious conversion efficiency decreased after 14 runs, more catalytic cycles were expected to test the recyclability.

As REC had good dispersion in aqueous solution, the recycle process involving centrifugal separation unavoidably resulted in the loss of the powder-state catalyst. Loading Fe_3O_4 , chitosan and AuNP on REC not only made it easier to separate the catalyst for recycle usage, but also enhanced the catalytic efficiency.

4. Conclusion

The REC- Fe_3O_4 -CTS-Au composite was fabricated by orderly introducing Fe_3O_4 , chitosan and AuNP catalyst onto the layers of raw REC. As the carrier, REC layers supported Fe_3O_4 particles, chitosan and AuNPs. The composite was easily recovered due to magnetic Fe_3O_4 particles, and hydroxyl groups of chitosan could form interaction with metal ions and prevent from the aggregate of nanoparticles to improve the dispersion and catalytic activity of the composite catalyst. The REC- Fe_3O_4 -CTS-Au composite was used to catalyze the reduction of 4-NP and MO in the presence of NaBH_4 . The REC- Fe_3O_4 -CTS-Au composite exhibited good catalytic capacity and magnetic recycling properties toward the reduction of 4-NP and MO, which made it a promising candidate in chemical and environmental application.

Acknowledgements

This research was supported by the National Nature Science Foundation of China (51462009).

References

- [1] D.L. Wu, P.W. Zheng, P.R. Chang, X.F. Ma, Preparation and characterization of magnetic rectorite/iron oxide nanocomposites and its application for the removal of the dyes, *Chem. Eng. J.* 174 (2011) 489-494.
- [2] W. Shi, Q. Cheng, P. Zhang, Catalytic decolorization of methyl orange by the rectorite-sulfite system, *Catal. Commun.* 56 (2014) 32-35.
- [3] Y. Huang, X.Y. Ma, G.Z. Liang, Adsorption behavior of Cr(VI) on organic-modified rectorite, *Chem. Eng. J.* 138 (2008) 187-193.
- [4] G.C. Han, Y. Han, X.Y. Wang, Synthesis of organic rectorite with novel Gemini surfactants for copper removal, *Appl. Surf. Sci.* 317 (2014) 35-42.
- [5] J.A. Johnson, J.J. Makis, K.A. Marvin, S.E. Rodenbusch, K.J. Stevenson, Size-dependent hydrogenation of p-nitrophenol with Pd nanoparticles synthesized with poly(amido)amine dendrimer templates, *J. Phys. Chem. C* 117 (2013) 22644-22651.
- [6] M.Y. Abdelaal and R.M. Mohame, Novel Pd/TiO₂ nanocomposite prepared by modified sol-gel method for photocatalytic degradation of methylene blue dye under visible light irradiation, *J. Alloys Compd.* 576 (2013) 201-207.
- [7] H.M. Lu and X.K. Meng, Size-, shape-, and dimensionality-dependent melting temperatures of nanocrystals, *J. Phys. Chem. C* 114 (2009) 1534-1538.
- [8] Y.H. Deng, Y. Cai, Z.K. Sun, J. Liu, C. Liu, J. Wei, W. Li, C. Liu, Y. Wang, D.Y. Zhao, Multifunctional mesoporous composite microspheres with well-designed nanostructure: a highly integrated catalyst system, *J. Am. Chem. Soc.* 132 (2010) 132,

8466-8473.

- [9] L.C. Zhou, Y.M. Shao, J.R. Liu, Z.F. Ye, H. Zhang, J.J. Ma, Y. Jia, W.J. Gao, Y.F. Li, Preparation and characterization of magnetic porous carbon microspheres for removal of methylene blue by a heterogeneous fenton reaction, *ACS Appl. Mater. Interfaces* 6 (2014) 7275-7285.
- [10] A.A. Ismail, A. Hakki, D.W. Bahnemann, Mesoporous Au/TiO₂ nanocomposites for highly efficient catalytic reduction of p-nitrophenol, *J. Mol. Catal. A- Chem.* 358 (2012) 145-151.
- [11] Y. Yu, Kant, J.G. Shapter, Gold nanotube membranes have catalytic properties, *Micropor. Mesopor. Mat.* 153 (2012) 131-136.
- [12] K. Kurada, T. Ishida, M. Haruta, Reduction of 4-nitrophenol to 4-aminophenol over Au nanoparticles deposited on PMMA, *J. Mol. Catal. A- Chem.* 298 (2009) 7-11.
- [13] Y. Li, X.B. Fan, J.J. Qi, Gold nanoparticles-graphene hybrids as active catalysts for Suzuki reaction, *Mater. Res. Bull.* 45 (2010) 1413-1418.
- [14] Y.Q. He, N. Zhang, L. Zhang, Fabrication of Au-Pd nanoparticles/graphene oxide and their excellent catalytic performance, *Mater. Res. Bull.* 51 (2014) 397-401.
- [15] M.Y. Tang, T. Wu, H.Y. Na, Fabrication of graphene oxide aerogels loaded with catalytic AuPd nanoparticles, *Mater. Res. Bull.* 63 (2015) 148-252.
- [16] S.J. Bae, S.J. Gim, H.J. Kim, Effect of NaBH₄ on properties of nanoscale zero-valent iron and its catalytic activity for reduction of p-nitrophenol, *Appl. Catal. B-Environ.* 182 (2016) 541-549.
- [17] Y.K. Cai, K.L. Gao, G.C. Li, Facile controlled synthesis of silver particles with

- high catalytic activity, *Colloid Surface A* 481 (2015) 407-412.
- [18] L.X. Zeng, M.J. Xie, Q.Y. Zhang, Chitosan/organic rectorite composite for the magnetic uptake of methylene blue and methyl orange, *Carbohydr. Polym.* 123 (2015) 89-98.
- [19] Y.J. Lu, P.R. Chang, P.W. Zheng, Porous 3D network rectorite/chitosan gels: Preparation and adsorption properties, *Appl. Clay Sci.* 107 (2015) 21-27.
- [20] W. Zuo, G.S. Chen, F.J. Chen, S.L. Li, B.D. Wang. Green synthesis and characterization of gold nanoparticles embedded into magnetic carbon nanocages and their highly efficient degradation of methylene blue. *Res advances* 6 (2016) 28774-28780.
- [21] Y.R. Zhang, S.L. Shen, S.Q. Wang, J. Huang, P. Su, Q.R. Wang, B.X. Zhao. A dual function magnetic nanomaterial modified with lysine for removal of organic dyes from water solution. *J. Ind. Eng. Chem.* 239 (2014) 250-256.
- [22] N. Pradhan, A. Pal, T. Pal, Silver nanoparticle catalyzed reduction of aromatic nitro compounds, *Colloid Surface A* 196 (2012) 247-257.
- [23] Y.Y. Zheng, J.X. Shu, Z.H. Wang, AgCl@Ag composites with rough surfaces as bifunctional catalyst for the photooxidation and catalytic reduction of 4-nitrophenol, *Mater. Lett.* 158 (2015) 339-342.
- [24] K. Bankura, D. Rana, M.R. Mollick, Dextrin-mediated synthesis of Ag NPs for colorimetric assays of Cu²⁺ ion and Au NPs for catalytic activity, *Int. J. Biol. Macromol.* 80 (2015) 309-316.
- [25] W.B. Wang, A.Q. Wang, Characterization and properties of superabsorbent

nanocomposites based on natural guar gum and modified rectorite, Carbohydr. Polym.

77 (2009) 891-897.

[26] P. Kannan, S.A. John, Synthesis of mercaptothiadiazole-functionalized gold nanoparticles and their self-assembly on Au substrate, Nanotechnology 19 (2008) 085602.

[27] S. Hsieh, B.Y. Huang, S.L. Hsieh, C.C. Wu, C.H. Wu, P.Y. Lin, Y.S. Huang, C.W. Chang, Green fabrication of agar-conjugated Fe₃O₄ magnetic nanoparticles, Nanotechnology 21 (2010) 445601.

[28] S. Luo, P.F. Qin, J.H. Shao, Synthesis of reactive nanoscale zero valent iron using rectorite supports and its application for Orange II removal, Chem. Eng. J. 223 (2013) 1-7.

[29] P.X. Zhao, X.W. Feng, D.S. Huang, Basic concepts and recent advances in nitrophenol reduction by gold- and other transition metal nanoparticles, Coordin. Chem. Rev. 287 (2015) 114-136.

[30] Y.Q. He, N.N. Zhang, Q.J. Gong, Metal nanoparticles supported graphene oxide 3D porous monoliths and their excellent catalytic activity, Mater. Chem. Phys. 134 (2012) 585-589.

[31] Y.Z. Ling, X.J. Zeng, W.R. Tan, Quaternized chitosan/rectorite/AgNP nanocomposite catalyst for reduction of 4-nitrophenol, J. Alloys Comp. 647 (2015) 463-470.

Figure captions

Figure 1. The fabrication process of REC-Fe₃O₄-CTS-Au catalyst.

Figure 2. SEM images of REC (a), REC-Fe₃O₄ (b), REC-Fe₃O₄-CTS (c) and REC-Fe₃O₄-CTS-Au (d); TEM images for REC-Fe₃O₄ (e) and REC-Fe₃O₄-CTS-Au (f).

Figure 3. X-ray diffraction peaks of REC, REC-Fe₃O₄, REC-Fe₃O₄-CTS and REC-Fe₃O₄-CTS-Au (1-10°) (a) and (10-80°) (b).

Figure 4. FTIR spectra (a) and TG curves (b) of REC, REC-Fe₃O₄, REC-Fe₃O₄-CTS and REC-Fe₃O₄-CTS-Au.

Figure 5. Magnetic behavior of REC-Fe₃O₄-CTS-Au at 300 K.

Figure 6. Catalytic mechanism of 4-NP and MO reduction.

Figure 7. Catalytic activity of REC-Fe₃O₄-CTS-Au toward 4-NP and MO. Time-dependent pictures for the reduction of 4-NP and MO (a); Time-dependent UV-Vis adsorption spectra for the reduction of 4-NP (b) and MO (c) in aqueous solution at 30°C. (4-NP and MO concentration: 0.4 mM; catalyst concentration: 150 mg/L)

Figure 8. Effect of the catalyst concentration and 4-NP concentration on the degradation of 4-NP.

Figure 9. Effect of the catalyst concentration and MO concentration on the degradation of MO.

Figure 10. The recyclability of REC-Fe₃O₄-CTS-Au catalysts for the degradation of 4-NP (a) and MO (b).

Figure

Figure 1

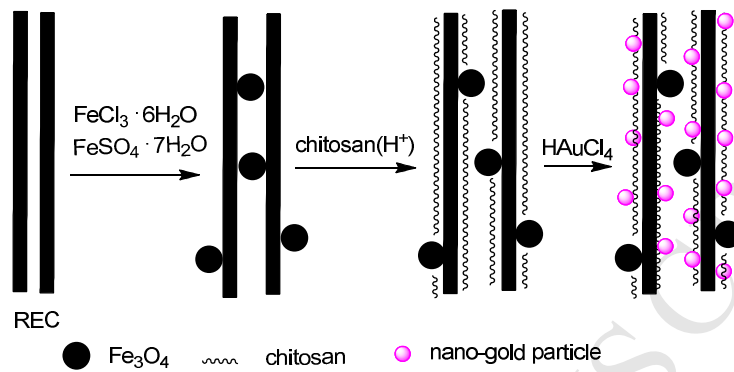


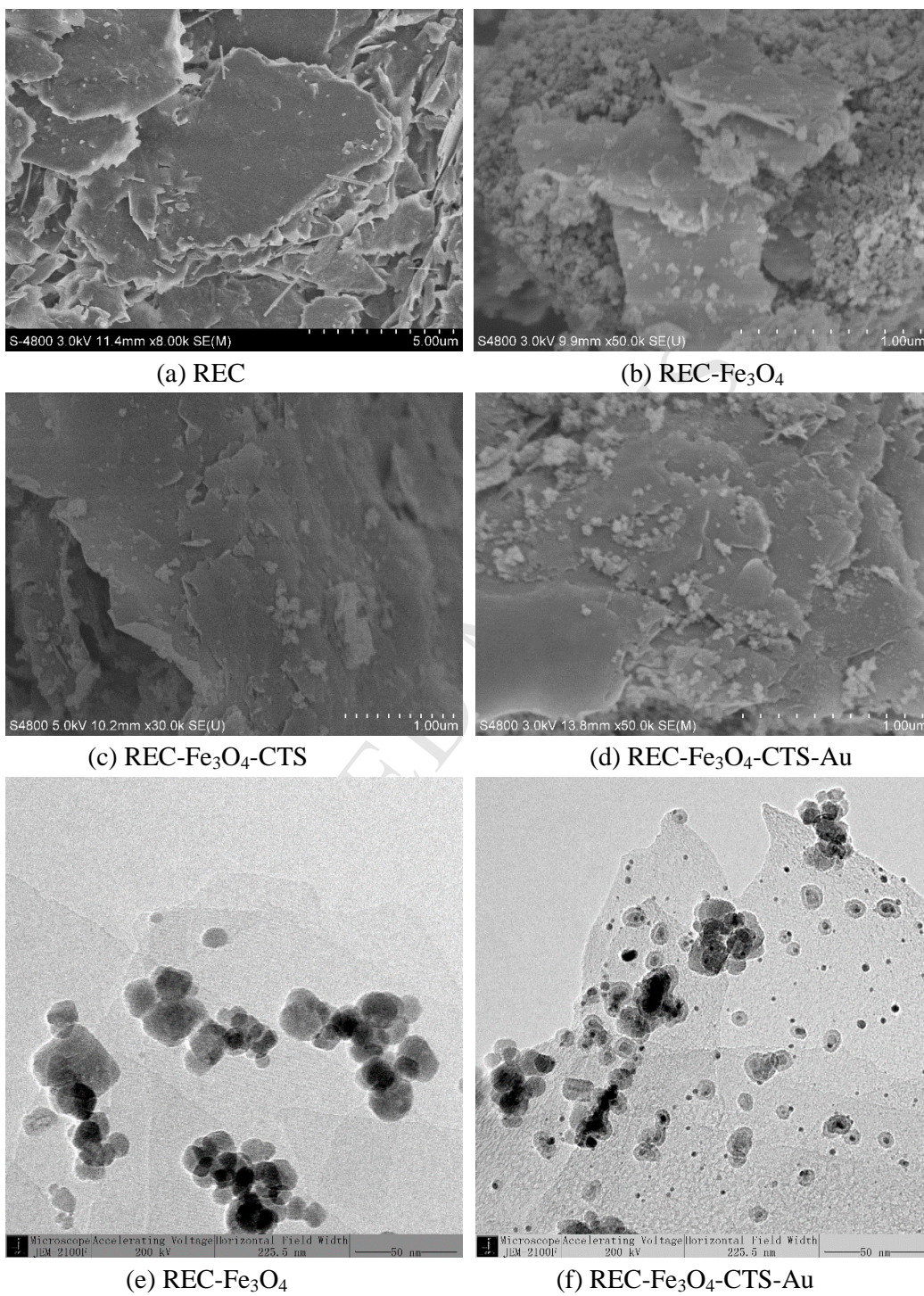
Figure 2

Figure 3

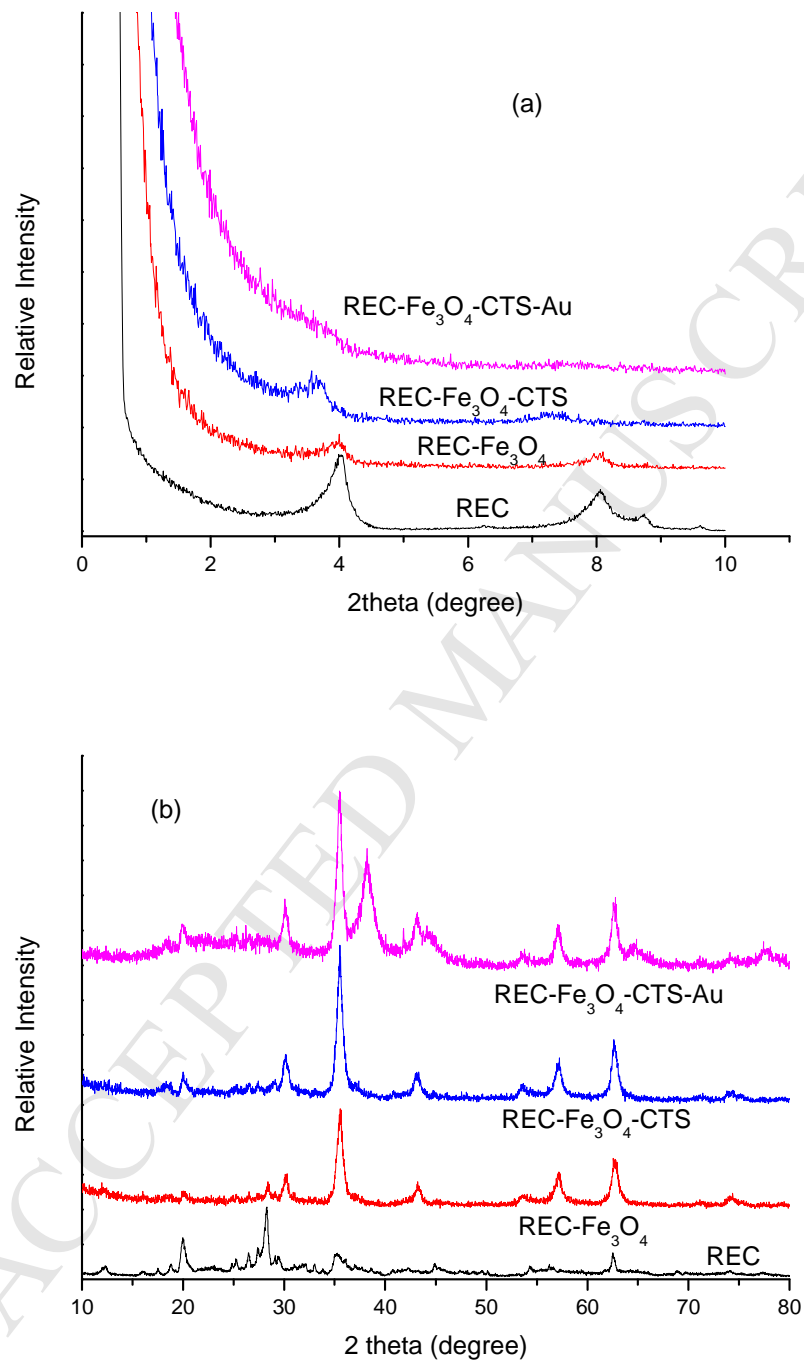


Figure 4

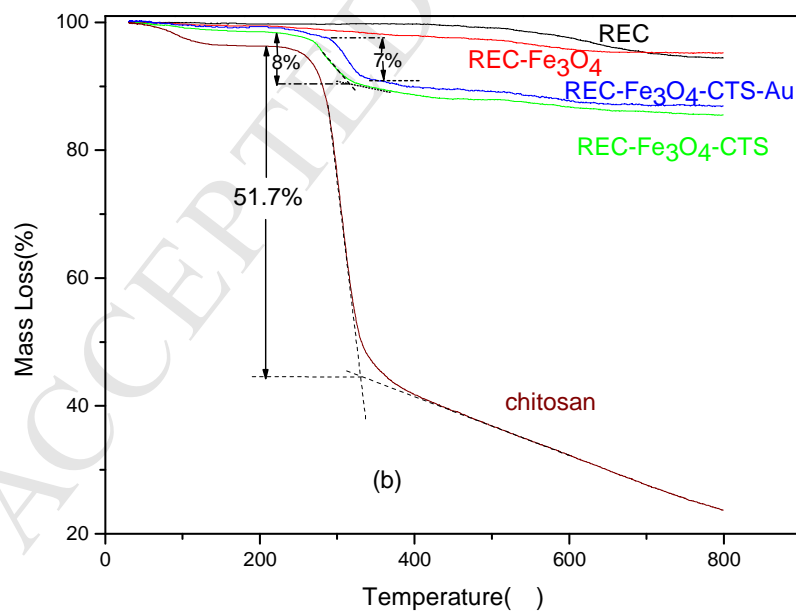
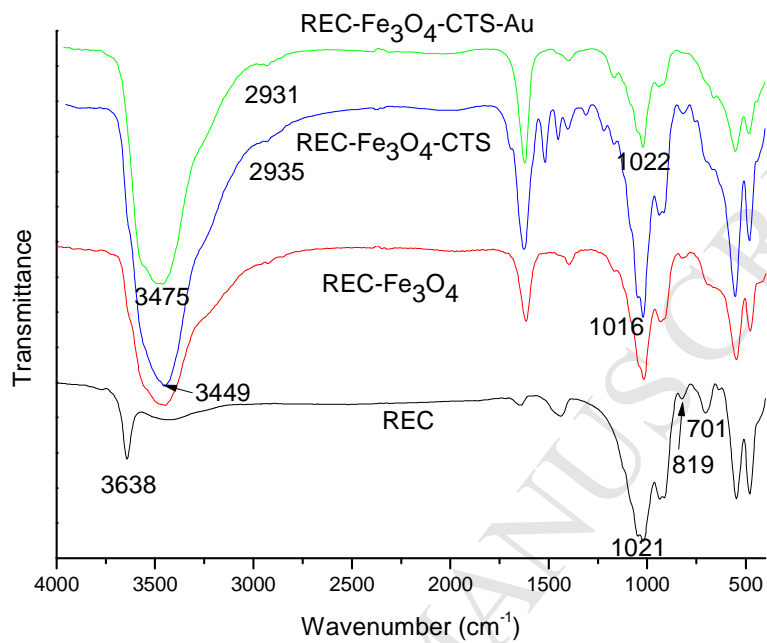


Figure 5

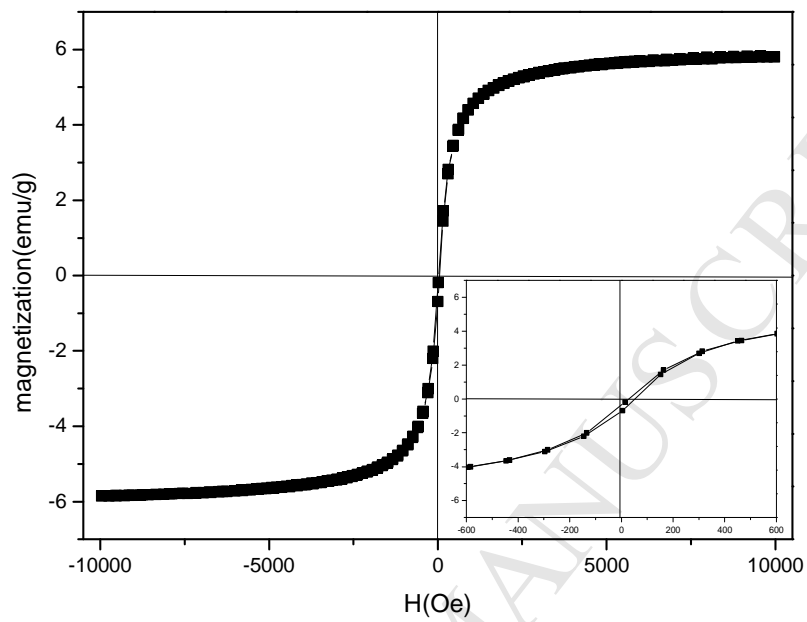


Figure 6

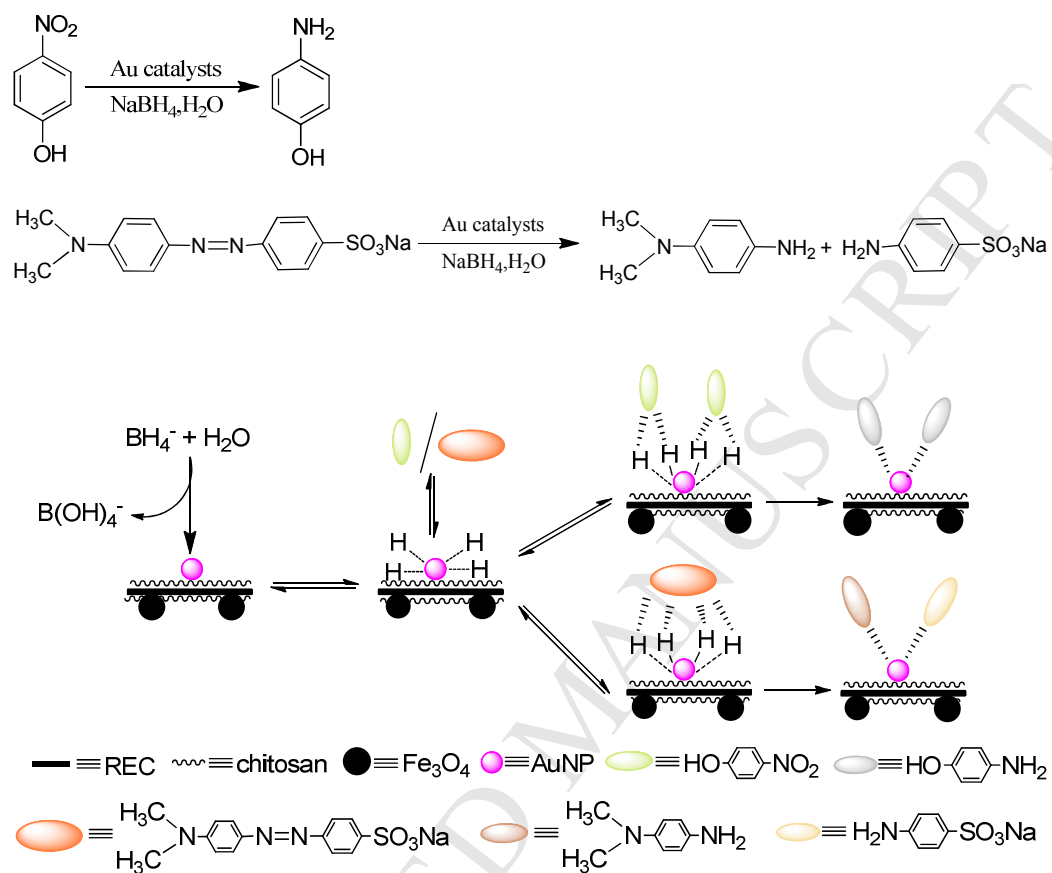
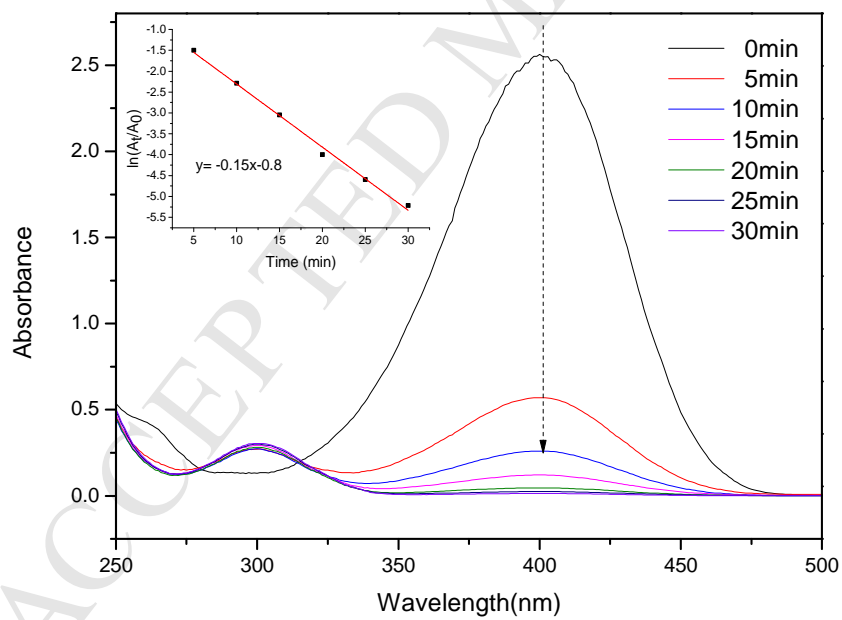
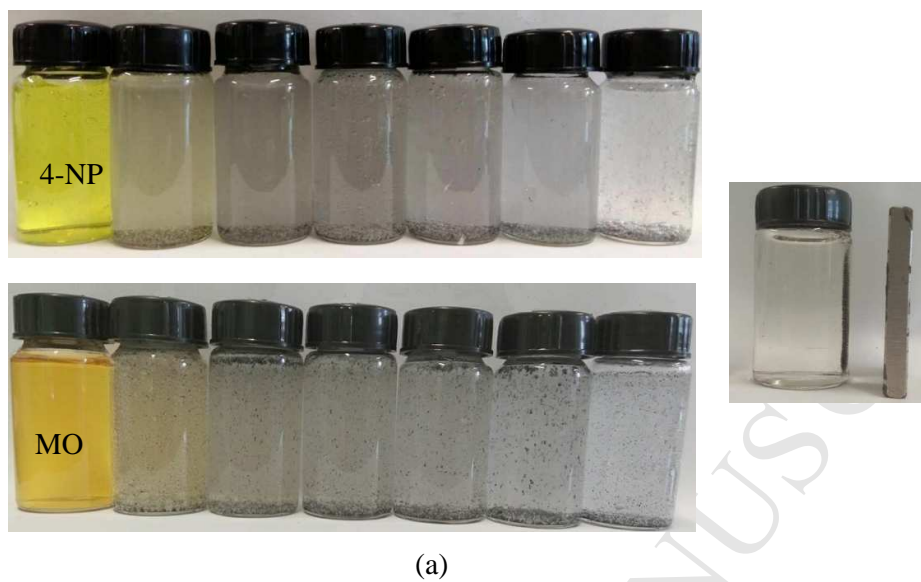


Figure 7



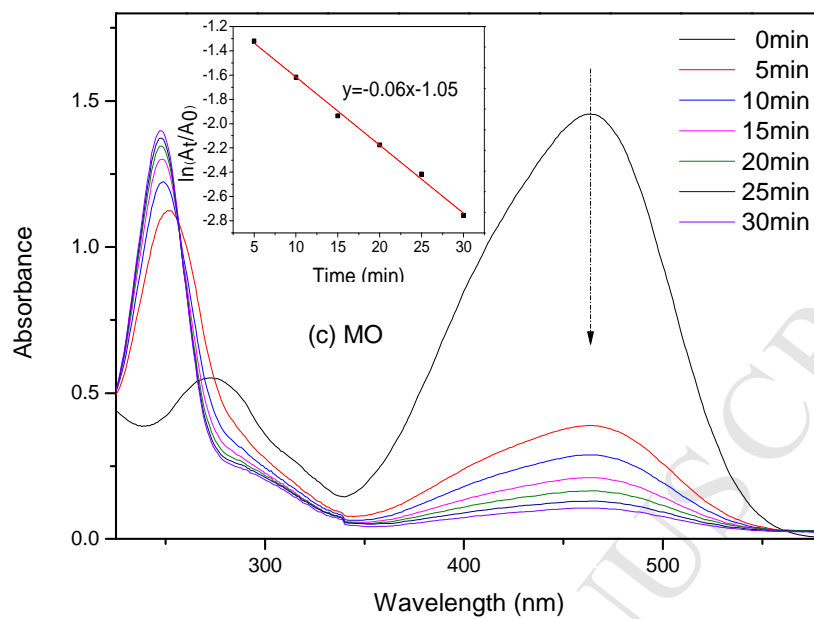
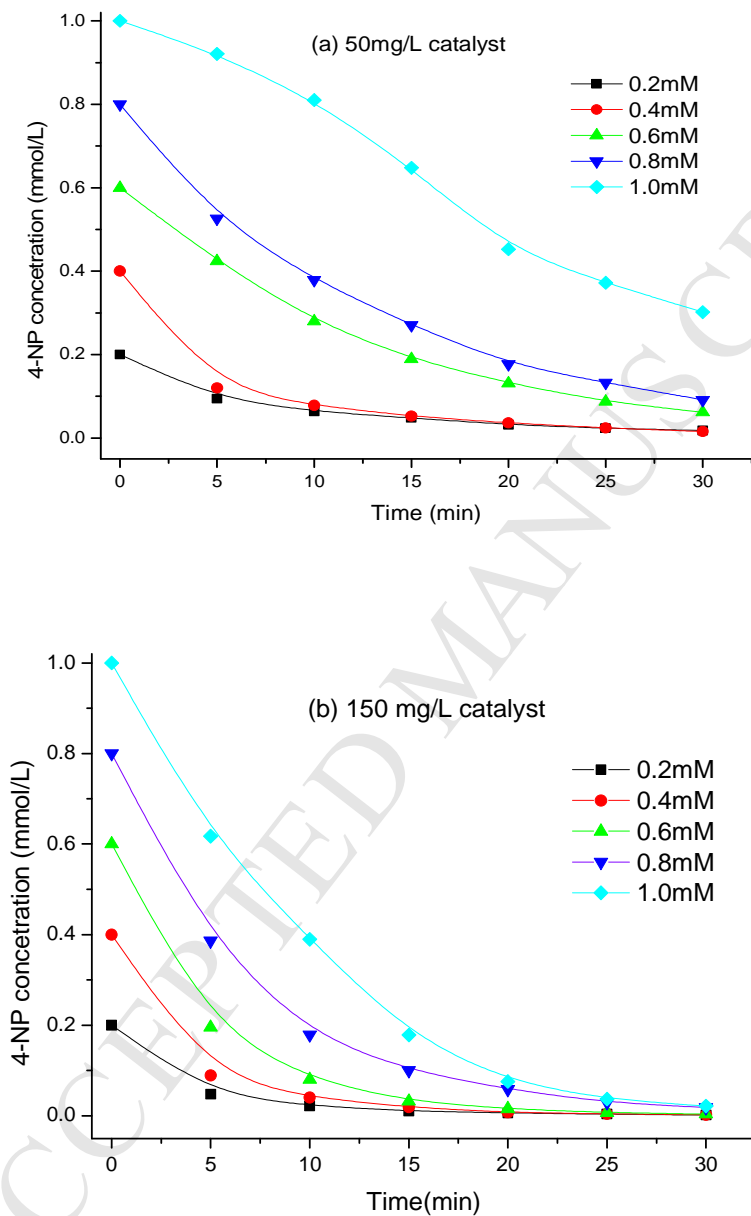


Figure 8



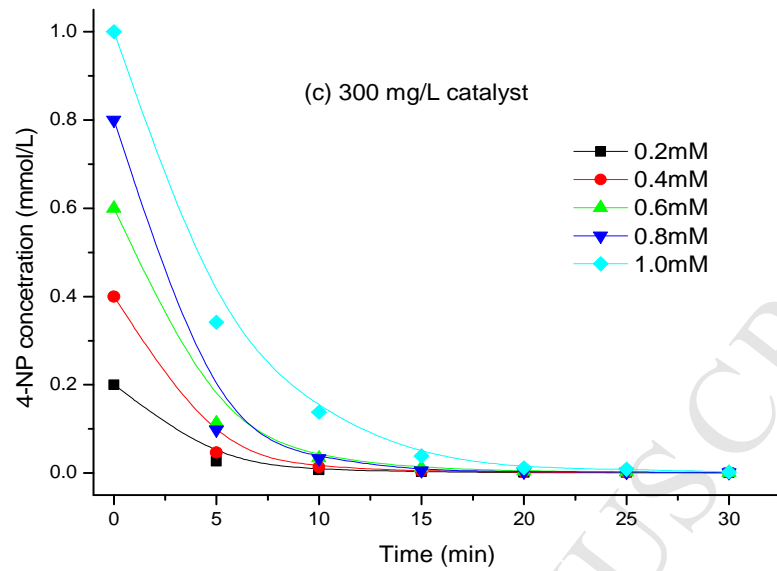
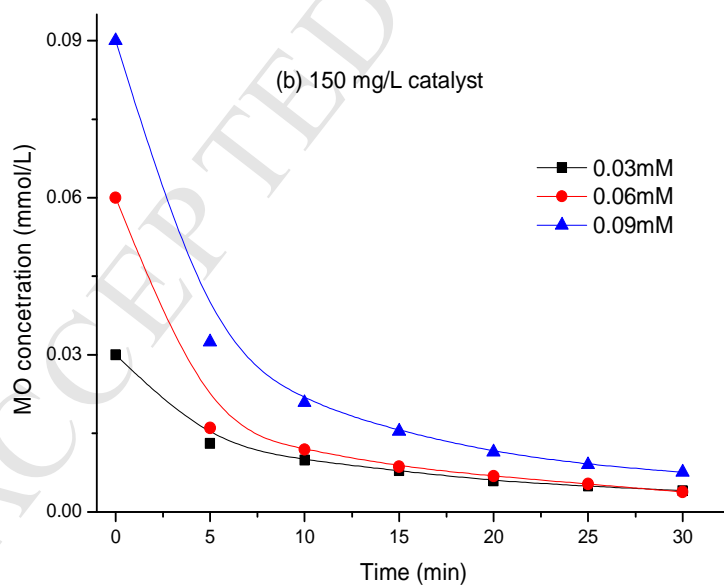
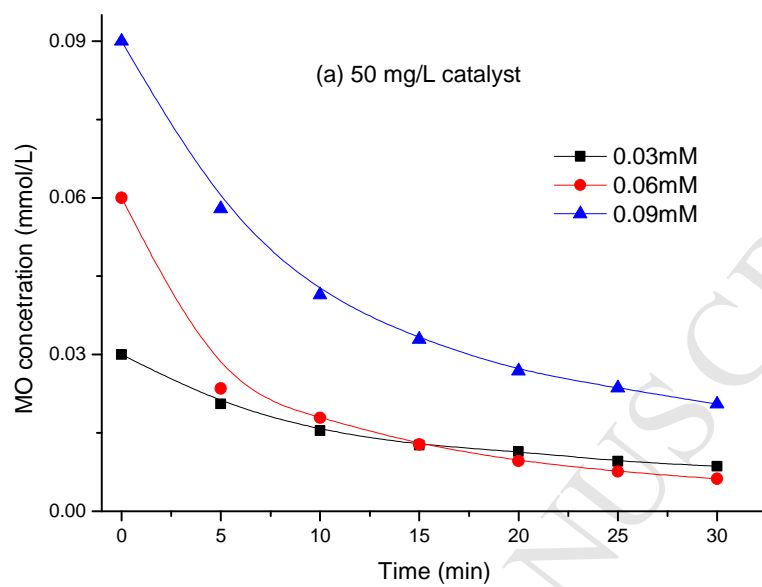


Figure 9



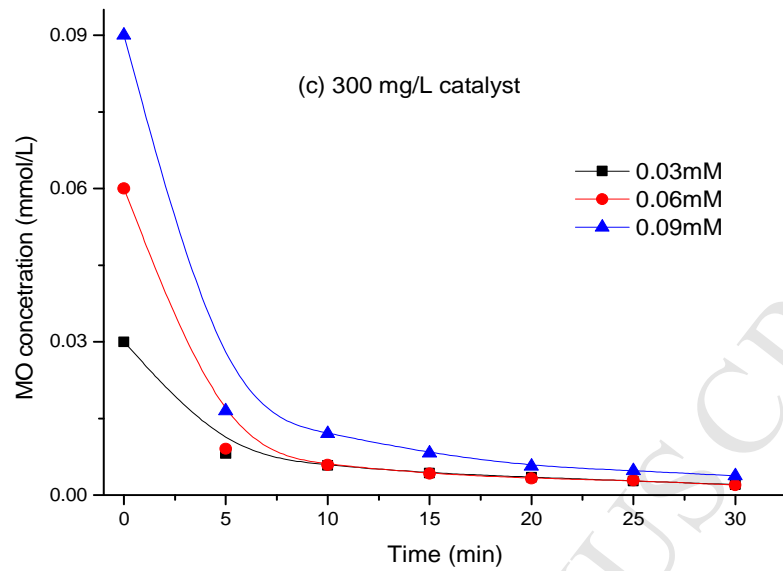
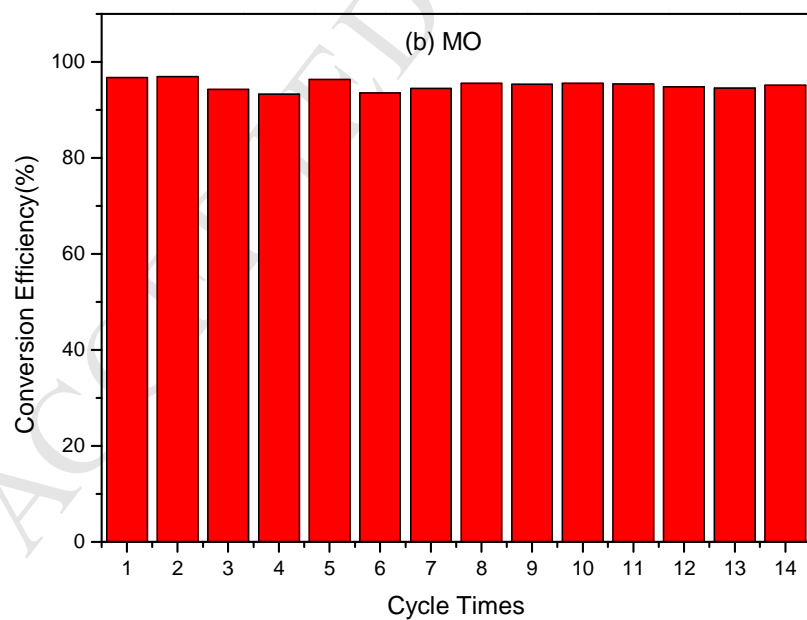
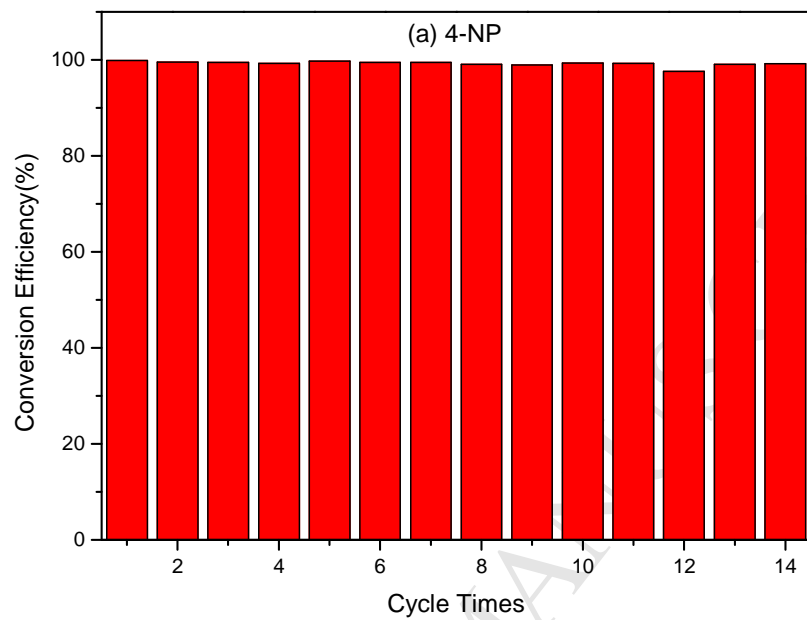


Figure 10



Highlights

- > REC-Fe₃O₄-CTS-Au was fabricated by orderly introducing Fe₃O₄, chitosan and AuNP.
- > The hydroxyl groups of chitosan prevented the aggregate of AuNPs to improve catalytic activity.
- > REC-Fe₃O₄-CTS-Au exhibited good catalytic capacity and recycle usage to the reduction of 4-NP and MO.